

Sonic Hedgehog Influences the Balance of Osteogenesis and Adipogenesis in Mouse Adipose-Derived Stromal Cells

Aaron W. James, B.A.,^{1,2,*} Philipp Leucht, M.D.,^{1,3,*} Benjamin Levi, M.D.,¹ Antoine L. Carre, M.D.,¹ Yue Xu, M.D., Ph.D.,¹ Jill A. Helms, Ph.D., D.D.S.,¹ and Michael T. Longaker, M.D., M.B.A.¹

Adipose-derived stromal cells (ASCs) present a great potential for tissue engineering, as they are capable of differentiating into osteogenic and adipogenic cell types, among others. In this study, we examined the role of Hedgehog signaling in the balance of osteogenic and adipogenic differentiation in mouse ASCs. Results showed that Hedgehog signaling increased during early osteogenic differentiation (*Shh*, *Ptc1*, and *Gli1*), but decreased during adipogenic differentiation. N-terminal Sonic Hedgehog (Shh-N) significantly increased *in vitro* osteogenic differentiation in mouse ASCs, by all markers examined ($*p < 0.01$). Concomitantly, Shh-N abrogated adipogenic differentiation, by all markers examined ($*p < 0.01$). Conversely, blockade of endogenous Hedgehog signaling, with the Hedgehog antagonist cyclopamine, enhanced adipogenesis at the expense of osteogenesis. We next translated these results to a mouse model of appendicular skeletal regeneration. Using quantitative real-time polymerase chain reaction and *in situ* hybridization, we found that skeletal injury (a monocortical 1 mm defect in the tibia) results in a localized increase in Hedgehog signaling. Moreover, grafting of ASCs treated with Shh-N resulted in significantly increased bone regeneration within the defect site. In conclusion, Hedgehog signaling enhances the osteogenic differentiation of mouse ASCs, at the expense of adipogenesis. These data suggest that Hedgehog signaling directs the lineage differentiation of mesodermal stem cells and represents a promising strategy for skeletal tissue regeneration.

Introduction

ADIPOSE-DERIVED STROMAL CELLS (ASCs) are a promising cell population for autologous tissue engineering.¹ Their ease of harvest, their relative abundance, and their capability for expansion make ASCs more attractive than other stromal cells for tissue regeneration. ASCs have a proven ability to differentiate into multiple mesodermal lineages, including osteoblastic and adipocytic cell fates.² An inverse relationship appears to exist between these two cell types, such that cytokines that enhance osteogenesis seem to repress adipogenic differentiation, and vice versa.^{3,4} These observations suggest that ASCs could be manipulated to adopt an osteoblast fate at the expense of an adipogenic one, given the appropriate cytokine stimulation. A small number of cytokines are known to enhance osteogenesis in mouse ASCs (mASCs), including bone morphogenetic proteins (BMPs), retinoic acid, and vitamin D.^{1,5} We have identified another

cytokine, Sonic Hedgehog (Shh), which potentially functions upstream of these known differentiation factors to induce osteogenesis in mASCs.

Hedgehog proteins, which include Sonic, Indian, and Desert, control numerous aspects of development and disease.⁶ Hedgehog signaling is initiated by the binding of the Hedgehog ligand to its transmembrane receptor patched1 (*Ptc1*), relieving suppression of the transmembrane protein smoothed (Smo). Smo activates an intracellular cascade that results in activation of Gli transcription factors.⁷ Hedgehog signaling exerts its pleiotropic effects through regulation of the cell cycle,⁸ direction of cell differentiation,⁹ and alteration of cell survival.¹⁰ Increased Hedgehog signaling promotes osteogenesis in various bone-forming cells *in vitro*.^{9,11–14} Conversely, Hedgehog signaling represses adipogenic differentiation in preadipocytes.^{15,16} Theoretically, the manipulation of Hedgehog signaling presents an attractive avenue for controlling the lineage commitment of ASCs in a tissue engineering strategy.

¹Hagey Pediatric Regenerative Medicine Laboratory, Division of Plastic and Reconstructive Surgery, Department of Surgery, Stanford University School of Medicine, Stanford, California.

²School of Medicine, University of California, San Francisco, California.

³Department of Orthopaedic Surgery, Stanford University School of Medicine, Stanford, California.

*These two authors contributed equally to this work.

We present a comprehensive analysis of the effects of Shh signaling in mASCs. First, we examined Hedgehog activity during osteo- and adipogenic differentiation. Next, we tested whether manipulation of Hedgehog signaling would influence mASC differentiation: N-terminal Shh (Shh-N) or the Hedgehog antagonist cyclopamine were added to osteogenic, adipogenic, or bipotent cell medium. The intersection of BMP and Hedgehog signaling was then examined. Finally, we exploited these *in vitro* findings in a novel strategy to accelerate bone regeneration following a surgically created defect in the mouse tibia (a monocortical defect in the proximal-medial tibia). Taken together, these data provide evidence that Hedgehog signaling favors the differentiation of mesodermal multipotent cells to an osteogenic lineage at the expense of an adipogenic one, and suggest a mechanism whereby the cell fate of ASCs can be directed for tissue engineering purposes.

Materials and Methods

Chemicals and supplies

Dulbecco's modified Eagle's medium and penicillin-streptomycin were purchased from Gibco Life Technologies, fetal bovine serum from Omega Scientific, recombinant Shh-N and recombinant BMP-2 from R and D Systems, and cell culture supplies from Corning, Inc.

Animals, tissue harvest, and primary cell culture

Mouse ASCs were isolated from fifty 3-week-old CD-1 mice (Charles River Laboratories) as previously described.¹⁷ For *in vivo* experiments, ASCs were isolated from CD-1 mice in which the green fluorescent protein (GFP) was linked to a β -actin promoter. ASCs were cultured in a standard growth medium (SGM), containing Dulbecco's modified Eagle's medium, 10% fetal bovine serum, and 100 IU/mL penicillin-streptomycin. ASCs of passage two were used for all assays, unless otherwise stated.

Cellular proliferation in vitro

Cell proliferation was assessed by cell counting. ASCs were seeded in 12-well plates at 10,000 cells/well and cultured in

SGM, replenished every other day with Shh-N, cyclopamine, or vehicle control. Counting was performed by hemocytometer from 1 to 7 days.

Adipogenic differentiation in vitro

For adipogenic differentiation, cells were plated at a density of 50,000 cells/well in 12-well dishes; adipogenic medium containing SGM, 10 μ g/mL insulin, 1 μ M dexamethasone, 0.5 mM methylxanthine, and 200 μ M indomethacin was supplemented with Shh-N, cyclopamine, or vehicle as a control, and was replenished every 3 days. Oil red O staining was performed at day 7 to assess lipid accumulation as previously described.¹⁷ RNA was isolated after 7 days to examine gene expression by quantitative real-time polymerase chain reaction (qRT-PCR) (*peroxisome proliferator-activated receptor- γ* [PPAR- γ]).

Osteogenic differentiation in vitro

For osteogenic differentiation, cells were plated at a density of 25,000 cells/well in 12-well dishes. ASCs were treated with the osteogenic differentiation medium (ODM) containing SGM, 100 μ g/mL ascorbic acid, and 10 mM β -glycerophosphate. ODM was supplemented with Shh-N, cyclopamine, recombinant (r)BMP-2, or vehicle control, and was replenished every 3 days.

To assess gene expression, RNA was isolated from 0 to 14 days of differentiation and examined by qRT-PCR. Specific primer sequences can be found in Table 1. Alkaline phosphatase (ALP) staining and quantification was performed from 0 to 14 days of differentiation, as previously described.¹⁸ Total ALP activity was assayed by measuring the *p*-nitrophenol formed from the enzymatic hydrolysis of *p*-nitrophenylphosphate, which was normalized to total protein quantity (Pierce). Alizarin red (AR) staining was performed from 0 to 14 days of differentiation.¹⁸ Staining was quantified by cetylpyridinium chloride extraction and measurement of absorbance at 570 nm using spectrophotometry.

Bipotent differentiation in vitro

For bipotent differentiation, cells were plated at a density of 35,000 cells/well in 12-well dishes and treated with a

TABLE 1. QUANTITATIVE POLYMERASE CHAIN REACTION GENES AND PRIMER SEQUENCES

Gene name	Forward primer sequence (5'-3')	Reverse primer sequence (5'-3')
<i>Bmp2</i>	GGGACCCGCTGTCTTCTAGT	TCAACTCAAATTCGCTGAGGAC
<i>Bmp4</i>	TTCTGGTAACCGAATGCTGA	CCTGAATCTCGGCGACTTTTT
<i>Col 1α</i>	AACCCGAGGTATGCTTGATCT	CCAGTCTTTCATTGCATTGC
<i>Dhh</i>	CTTGGCACTCTTGGCACTATC	GACCCCTTGTTACCTCC
<i>Gapdh</i>	AGGAGTATATGCCGACGTG	TCGTCCACATCCACACTGTT
<i>Gli1</i>	TCGACCTGCAAACCGTAATCC	TCCTAAAGAAGGGCTCATGGTA
<i>Gli2</i>	GGCAGGGGTATCCACAGA	AGAAGGACCCATGTTGGAGTC
<i>Gli3</i>	CACAGTCTAGGCGACTG	CTGCATAGTGATTGCGTTTCTTC
<i>Ihh</i>	GCTTCGACTGGGTGTATTACG	GCTCGGGTCCAGGAAAAT
<i>Oc</i>	GGGAGACAACAGGGAGGAAAC	CAGGCTTCTGCCAGTACCT
<i>Opn</i>	AGCAAGAACTCTTCCAAGCAA	GTGAGATTCGTGATTCATCCG
PPAR- γ	TCGCTGATGCACTGCCTATG	GAGAGGTCCACAGAGCTGATT
<i>Ptc1</i>	GCCAAGCCCTAAAAAAT	ACCACAATCAACTCTCTG
<i>Runx2</i>	CGGTCTCCTTCCAGGATGGT	GCTTCCGTGAGCGTCAACA
<i>Shh</i>	AAAGCTGACCTTTAGCCTA	TTCGGAGTTTCTTGTGATCTTCC
<i>Smo</i>	GAGCGTAGCTTCCGGGACTA	CTGGGCCGATTCTTGATCTCA

bipotent medium, including components of both ODM and adipogenic medium. The medium supplemented with Shh-N, cyclopamine, or vehicle control was replenished every 3 days. After 7 days, oil red O staining was performed, followed by ALP staining on the same well.

RNA isolation and qRT-PCR

RNA isolation was performed as previously described.¹⁸ Isolation was performed with the RNeasy Mini Kit (Qiagen Sciences). After DNase treatment, reverse transcription of 1 µg RNA was performed with TaqMan Reverse Transcription Reagents (Applied Biosystems). qRT-PCR was carried out using the Applied Biosystems Prism 7900HT Sequence Detection System and Power SYBR Green Master Mix (Applied Biosystems). All PCR products were run out on a 2% agarose gel to determine appropriate size and specificity. Sequences are shown in Table 1. Levels of expression were determined by normalizing to *GAPDH*; reactions were performed in triplicate.

ASC grafting of mouse tibial defects

Upon subconfluency, passage 0 ASCs derived from GFP transgenic mice were treated with Shh-N or vehicle control for 24 h (500 ng/mL). Cells were then trypsinized, centrifuged, and resuspended at a concentration of 10,000 cells/µL. All procedures were approved by the Stanford Committee on Animal Research. Skeletally mature (10 weeks of age) male CD-1 mice were used. After anesthesia and analgesia, the right leg was shaved and cleansed. Briefly, to gain access to the anterior aspect of the tibia, the tibialis anterior muscle was elevated off the periosteum. Care was taken to avoid damage to the tibial periosteum, as this is known to cause a host osteogenic response. Next, the tibial surface was rapidly washed with sterile phosphate-buffered saline, and a drill hole was created through a single cortex (monocortical) in the midline of the tibia just distal to the tibial tuberosity using a dental drill (NSK z500; Brasseler). The far cortex was neither touched nor penetrated by the drill, verified by histologic analysis. Moreover, the integrity of the surrounding bone was maintained such that no fractures occurred, again verified by histologic analysis. After phosphate-buffered saline irrigation, 1 µL of a cell suspension was placed into the injury site, using a 2 µL pipette and sterile pipette tip. To ensure that the cells were contained in the defect, the muscle belly of the tibialis anterior was flipped back over the anterior surface to cover the defect site. To maintain its anatomic position, a single 6-0 Prolene suture (Ethicon) was placed through the tibialis anterior muscle into the gastrocnemius–soleus muscle complex. This technique allowed for a confined space in which the grafted cells remained in place and reduced potential hematoma formation. Finally, the region was lastly irrigated and the skin closed with 7-0 Prolene (Ethicon). In our previous study, we ensured successful cell engraftment by both GFP labeling and *in vivo* imaging of Luciferase activity.¹⁹

Tissue harvest

Samples were harvested at postoperative day 6 to examine early callus formation. Samples were fixed in 0.4% paraformaldehyde overnight, and decalcified in 19% ethylenediaminetetraacetic acid for 12 days. Samples were dehydrated in

a graded ethanol, paraffin embedded, and sectioned at 8 µm thickness. Gene expression in the developing callus was assessed by qRT-PCR. On postoperative days 1–7, the injury site was dissected with a minimal border of uninjured tibia. Tissue samples were pooled, snap-frozen, and homogenized with mortar and pestle, followed by RNA isolation and gene analysis (*Gli1*, *Smo*, and *Ptc1*).

Standard histological assays

Histology was performed using a modification of the Movat's Pentachrome and Aniline Blue stains. ALP staining was performed using 5M NaCl, 1M Tris-HCl (pH 9.5), 1M MgCl₂, 0.1% Tween 20% (NTMT) ALP buffer and nitro blue tetrazolium chloride (NBT) and 5-bromo-4-chloro-3-indolyl phosphatase (BCIP) for color (Roche). For GFP immunohistochemistry, slides were immersed in 0.3% H₂O₂/Methanol; blocked in milk, bovine serum albumin, and sheep serum; and incubated with a rabbit polyclonal anti-GFP primary antibody (Abcam) overnight at 4°C. A peroxidase-conjugated secondary antibody was used (Jackson ImmunoResearch), followed by diaminobenzadine for color development (Vector-Lab). Bromodeoxyuridine immunohistochemistry was performed according to the manufacturer's instructions (Zymed). To detect BMP activity within the defect site, immunohistochemistry for phospho-Smad 1/5/8 was performed. After peroxidase quenching, blocking was performed in donkey serum, followed by incubation with rabbit polyclonal primary antibody for 1 h at room temperature, biotinylated secondary antibody, followed by Vectastain and diaminobenzadine for color detection. To detect Hedgehog pathway activity, *in situ* hybridization for *Ptc1* was performed as previously described.²⁰ Briefly, the template was amplified from embryonic mouse cDNA by PCR using sequence-specific primers that included the T3 RNA polymerase. Antisense riboprobe was transcribed with T3 RNA polymerase in the presence of Dig-11-UTP (Roche). Sections were incubated for 12 h in hybridization buffer (Ambion) containing riboprobe at ~0.2–0.3 µg/mL probe/kb of probe complexity. Slides were blocked with 10% sheep serum, 1% Boehringer-Mannheim Blocking Reagent (Roche), and levamisole, and developed using NBT and BCIP for color.

Histomorphometric analyses of bone regeneration

Histomorphometry was accomplished by comparison of control and Shh-N-treated ASC injury sites. Tissue sections were stained with Aniline Blue. In total, eight animals were used for each condition. The injury site was represented across ~50 tissue sections. Of these, 10–15 tissue sections were used for histomorphometric measurements. Each section was photographed using a Leica digital imaging system (5×objective). The digital images were imported into Adobe Photoshop CS2. The number of Aniline-blue-stained pixels was determined using the magic wand tool (tolerance setting; 60, histogram pixel setting; cache level 1) by a single blinded investigator, and confirmed by a second independent investigator. These data were then used to calculate the average new bone in each injury site.

Statistical analyses

Means and standard deviations were calculated from all numerical data. In graphs, all bars represent means, whereas

all error bars represent one standard deviation. Statistical analyses were performed using the Welch's two-tailed *t*-test when comparing two groups with unequal standard deviations. When comparing multiple groups, a one-way ANOVA test without replication was performed, followed by *post hoc* analysis using the Bonferroni correction to adjust for multiple comparisons. **p* < 0.01 was considered significant, unless otherwise stated.

Results

Endogenous Hedgehog signaling during mASC differentiation

Mouse ASCs can adopt either an osteogenic or adipogenic cell fate by exposure to the differentiation medium. We examined the time course of osteogenic differentiation using ALP activity to identify the onset of mineralization, and AR staining to identify calcified matrix (Fig. 1A). After 1 week in ODM, ALP activity was upregulated. After 2 weeks, ALP activity decreased, whereas AR staining increased substantially. Culture in adipogenic conditions led to lipid droplet formation by 1 week, shown by oil red O staining (Fig. 1C).

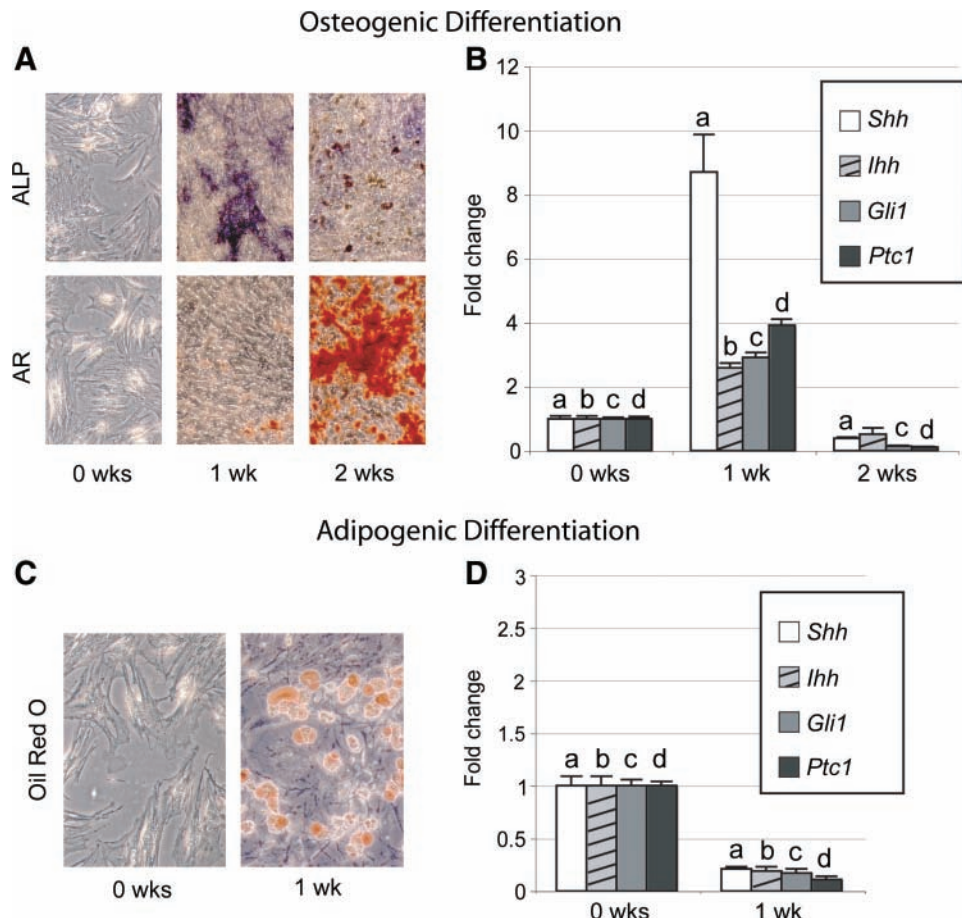
Next, we analyzed Hedgehog pathway activity during osteo- and adipogenic differentiation (Fig. 1B, D). Using qRT-PCR, all Hedgehog ligands were detected in mASCs, including Sonic, Indian, and Desert Hedgehog (*Dhh* not shown). After 1 week in ODM, *Shh* expression increased 8-fold, while

Ihh increased 2.5-fold (Fig. 1B). *Dhh* expression remained unchanged (data not shown). Upregulation in the Hedgehog ligands was accompanied by upregulation in the Hedgehog target genes *Gli1* and *Ptc1* (Fig. 1B). *Gli2* and *Gli3* were either repressed or unchanged (data not shown). After 2 weeks in ODM, expression of Hedgehog ligands and other signaling components had decreased (Fig. 1B). In contrast, Hedgehog signaling components decreased in expression during adipogenic differentiation after 7 days (Fig. 1D). These results demonstrate that the Hedgehog pathway is active in mASCs, and that osteogenic differentiation is accompanied by Hedgehog pathway activation.

mASC response to exogenous Hedgehog stimulation

We next tested how mASCs responded to an exogenous Hedgehog stimulus. Using qRT-PCR, we found that Shh-N treatment resulted in a dose-dependent increase in *Gli1* and *Ptc1* transcripts by 48 h (Fig. 2A). *Gli2* and *Gli3* were upregulated to a lesser degree. Thus, mASCs possess the molecular machinery necessary to process an exogenous Hedgehog stimulus. Next, Hedgehog ligand expression was evaluated after treatment with exogenous Hedgehog protein. Shh-N addition increased *Shh* transcripts at 48 h (Fig. 2B). No significant change in *Ihh* or *Dhh* expression was observed. Thus, a positive regulatory feedback system was observed, such that exogenous Hh treatment increased endogenous Hh expression.

FIG. 1. Hedgehog signaling during osteogenic and adipogenic differentiation. (A) Progression of mouse adipose-derived stromal cell (ASC) osteogenic differentiation through 2 weeks, shown by alkaline phosphatase (ALP) and alizarin red (AR) staining. (B) Sonic Hedgehog (*Shh*), Indian Hedgehog (*Ihh*), *Gli1*, and patched (*Ptc1*) expression at 0, 1, and 2 weeks of osteogenic differentiation, normalized to *GAPDH*. (C) Mouse ASC adipogenic differentiation, shown by oil red O staining. (D) *Shh*, *Ihh*, *Gli1*, and *Ptc1* expression at 0 and 1 week of adipogenic differentiation, normalized to *GAPDH*. Photographs are of 20× magnification; means and significance levels are calculated relative to 0 week expression, ^{a,b,c,d}*p* < 0.01. Color images available online at www.liebertonline.com/ten.



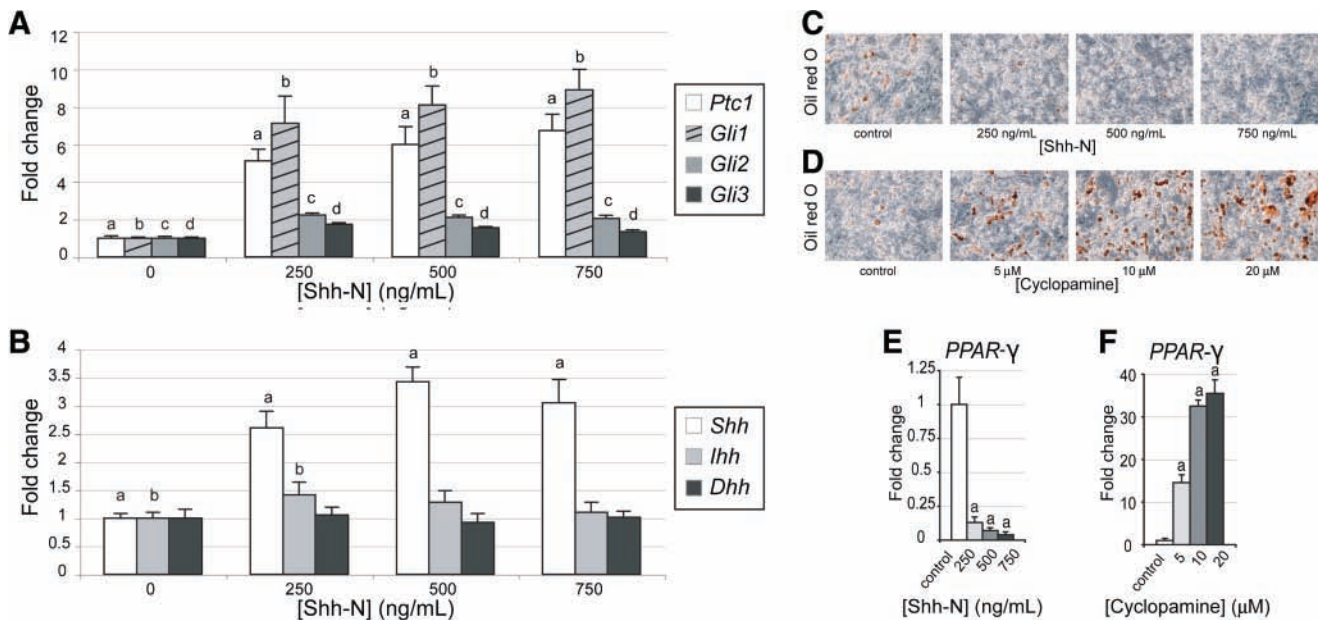


FIG. 2. Hedgehog pathway activation and adipogenic differentiation in ASCs. (A) Hedgehog signaling elements following culture with N-terminal Sonic Hedgehog (Shh-N) for 48 h by quantitative real-time polymerase chain reaction (qRT-PCR), including *Ptc1*, *Gli1*, *Gli2*, and *Gli3*. (B) Hedgehog ligand expression after Shh-N exposure for 48 h, including *Shh*, *Ihh*, and *Dhh*. (C–F) Adipogenic differentiation with Shh-N or cyclopamine. (C) Oil red O staining with Shh-N at day 7 adipogenic differentiation (250–750 ng/mL). (D) Oil red O staining with cyclopamine at day 7 differentiation (5–20 μM). (E) *PPAR-γ* expression with Shh-N at 7 days, by qRT-PCR. (F) *PPAR-γ* expression with cyclopamine at 7 days of differentiation. Means and significance levels are calculated relative to control expression levels, ^{a,b,c,d} $p < 0.01$. Color images available online at www.liebertonline.com/ten.

Hedgehog signaling represses adipogenic differentiation in mASCs

We next explored the response of mASCs to Hedgehog stimulation. Cells were cultured in adipogenic conditions, and treated with Shh-N or the Hedgehog antagonist, cyclopamine (Fig. 2C–F). Lipid accumulation was assessed by oil red O staining after 7 days. Under control conditions, mASCs exhibited lipid accumulation (red staining), reduced with addition of Shh-N (Fig. 2C). Shh-N also caused a dose-dependent decrease in *PPAR-γ* expression (Fig. 2E). The negative effect of Shh-N on adipogenic differentiation could not be explained by impaired cell proliferation, as proliferation assays showed a slight mitogenic response to Shh-N (data not shown). Thus, Shh-N treatment resulted in activation of the Hedgehog pathway, repression of adipogenic gene expression, and inhibition of adipogenic differentiation.

We next repressed endogenous Hedgehog activity with Hedgehog antagonist cyclopamine and assessed adipogenesis. mASCs exposed to cyclopamine showed a significant increase in lipid accumulation (Fig. 2D). *PPAR-γ* expression increased over 35-fold with cyclopamine addition to the medium (20 μM, Fig. 2F). Taken together, these data suggested that the endogenous Hedgehog pathway functions to repress the adipogenic differentiation of mASCs, and that cyclopamine is sufficient to induce adipocyte differentiation.

Hedgehog signaling enhances osteogenic differentiation of mASCs

Adipogenesis and osteogenesis appear to be dichotomous cell fates; we tested the extent to which Hedgehog regulates

this decision. mASCs were cultured in ODM with Shh-N for various periods (Fig. 3). By day 4, qRT-PCR data demonstrated that Shh-N elicited a dose-dependent increase in *Runx2* and collagen type I (*Col1*) expression levels (Fig. 3A). By day 7, Shh-N treatment resulted in a dose-dependent increase in ALP staining, which was confirmed by ALP quantification assays (Fig. 3B). By day 14, Shh-N treatment of mASCs induced mineralization, and a colorimetric quantification revealed that Shh-N increased AR staining in a dose-dependent manner (Fig. 3C). Also by day 14, Shh-N significantly increased osteopontin (*Opn*) and osteocalcin (*Oc*) gene expression relative to control, by qRT-PCR (Fig. 3D).

We hypothesized that endogenous Hedgehog production in mASCs also stimulated osteogenesis. To test this we blocked Hedgehog activity by including cyclopamine in ODM (Fig. 4). mASCs exposed to cyclopamine showed a significant decrease in *Runx2* and *Col1* expression on day 4 (Fig. 4A), and a significant decrease in AR staining (Fig. 4C). Thus, cyclopamine significantly impaired osteogenic differentiation, suggesting the necessity of endogenous Hedgehog signaling for the normal progression of mASC differentiation to an osteogenic fate.

To confirm that Shh-N was sufficient to enhance osteogenic differentiation, a combination of Shh-N and cyclopamine was added to ODM. Shh-N alone significantly increased all markers of osteogenesis, including an increase in *Runx2* and *Col1α1* expression, as well as increased ALP activity and AR staining (Fig. 4A–C). The introduction of cyclopamine abrogated this Hedgehog-induced increase in osteogenic markers (Fig. 4A–C).

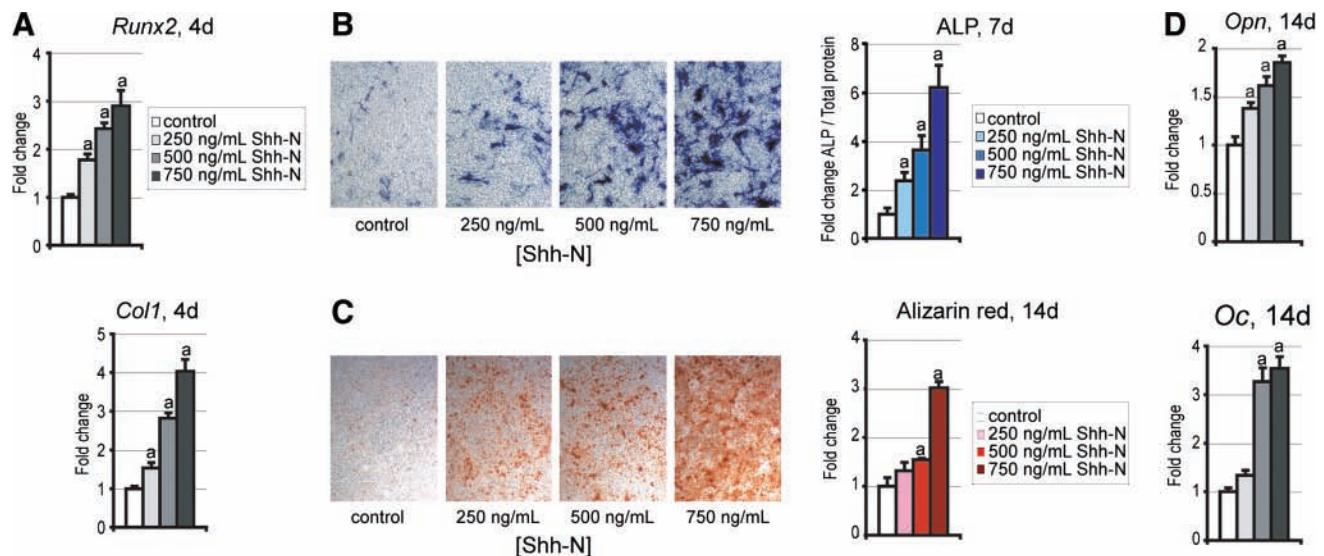


FIG. 3. Osteogenic differentiation with Shh-N. Osteogenic differentiation was examined through a 14 day time course. (A) *Runx2* and collagen type I (*Col1*) expression by qRT-PCR after 4 days. (B) ALP staining after 7 days, appearing blue. ALP quantification after 7 days was normalized to total protein content. (C) AR staining and quantification after 14 days. (D) Osteopontin (*Opn*) and Osteocalcin (*Oc*) expression by qRT-PCR after 14 days. Photographs are of 20 \times magnification; values are normalized to control expression levels, ^a $p < 0.01$. Color images available online at www.liebertonline.com/ten.

Effects of Hedgehog signaling in bipotent differentiation of mASCs

Our results thus far indicated that Hedgehog signaling functions in mASCs to influence cell differentiation toward an osteoblast cell fate at the expense of an adipocytic one. To directly test this, mASCs were cultured in the bipotent differentiation medium with either Shh-N or cyclopamine added (Supplemental Fig. S1, available online at www.liebertonline.com/ten). After 7 days of differentiation, both ALP and oil red O staining were performed. Shh-N robustly enhanced ALP staining, while lipid droplets were few in number (Supplemental Fig. S1A). The converse effect was observed with cyclopamine: ALP staining was minimal, while lipid formation was enhanced (Supplemental Fig. S1B). Collectively, these data demonstrate that Hedgehog activity was both necessary and sufficient for the induction of osteogenesis and for the repression of adipogenesis in mASCs.

Cooperative effect of Hedgehog and BMP-2 in osteogenic differentiation

BMP signaling has previously been observed to be necessary for mASC osteogenic differentiation⁵; we next sought to determine the intersection of Hedgehog and BMP signaling. Two days of treatment with Shh-N increased transcript abundance for *Bmp2* and *Bmp4* in a dose-dependent manner (Fig. 5A). Conversely, 2 days of treatment with rBMP-2 increased *Runx2* expression independent of a detectable increase in transcript levels of Hedgehog ligands or signaling components (Fig. 5B, *Ihh*, *Gli2*, and *Gli3* not shown). Thus, Shh-N positively regulated the transcription of osteogenic BMPs.

Next, Shh-N and rBMP-2 were added in combination to assess their potentially cooperative effects in mASC osteogenic differentiation. As expected, both rBMP-2 and Shh-N

when added to ODM alone induced ALP activity after 7 days (Fig. 5C). In combination, the two cytokines induced ALP activity in an additive fashion. Similar results were obtained with AR staining (Fig. 5D).

In vivo grafting of mASCs for skeletal regeneration

We extended our *in vitro* findings to an animal model of tissue regeneration, by directly testing the extent to which Hedgehog-stimulated ASCs could be used to repair a bony defect. First, we ascertained the endogenous level of Hedgehog activity that is induced in response to skeletal injury. A 1 mm skeletal defect was produced in a single cortex of the medial aspect of the proximal tibia of the mouse. We then used qRT-PCR to temporally map the pattern of Hedgehog responsiveness in the callus injury site from 1 to 7 days postoperatively (Fig. 6A). Hedgehog responsive genes, including *Gli1*, *Smo*, and *Ptc1*, were significantly increased after injury, with a peak in expression after 5 days. Injury-induced activation of these Hedgehog genes was specific to the injury site, as shown by *in situ* hybridization mapping of *Ptc1* (Fig. 6B, postoperative day 6 shown). Thus, skeletal injury stimulated endogenous Hedgehog activity, and it was into this environment that we grafted mASCs.

For the next series of experiments, mASCs were derived from *beta actin*:GFP mice. This strategy allowed us to distinguish the grafted mASCs and their progeny in the skeletal injury site. mASCs were harvested and cultured for 24 h in SGM supplemented with Shh-N (500 ng/mL) or vehicle control (Fig. 6C). After only 24 h, Shh-N-treated mASCs showed increased transcripts of *Runx2*, *Col1*, and *Bmp2* in comparison to control (Supplemental Fig. S2, available online at www.liebertonline.com/ten). Equal numbers of cells were grafted into a 1 mm monocortical tibial defect. On day 6, the callus sites were harvested for analysis, a time point

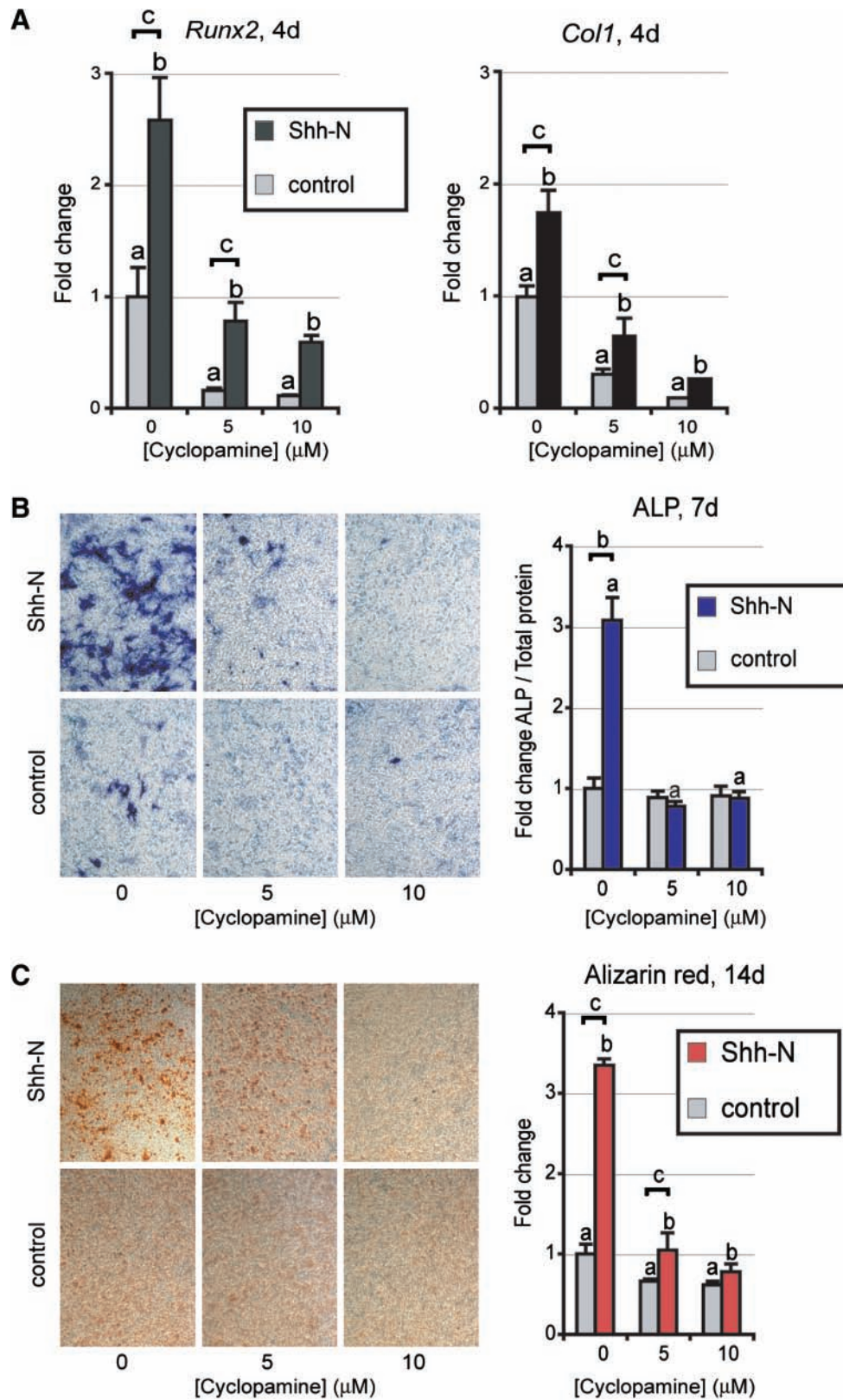


FIG. 4. Osteogenic differentiation of ASCs with cyclopamine. (A) *Runx2* and *Col1* expression with cyclopamine and/or Shh-N (500 ng/mL) at 4 days of differentiation, by qRT-PCR. (B) ALP staining and quantification with cyclopamine and/or Shh-N after 7 days. (C) AR staining and quantification with cyclopamine and/or Shh-N after 14 days. Photographs are of 20 \times magnification; values are normalized to control expression levels, ^{a,b,c}*p* < 0.01. Color images available online at www.liebertonline.com/ten.

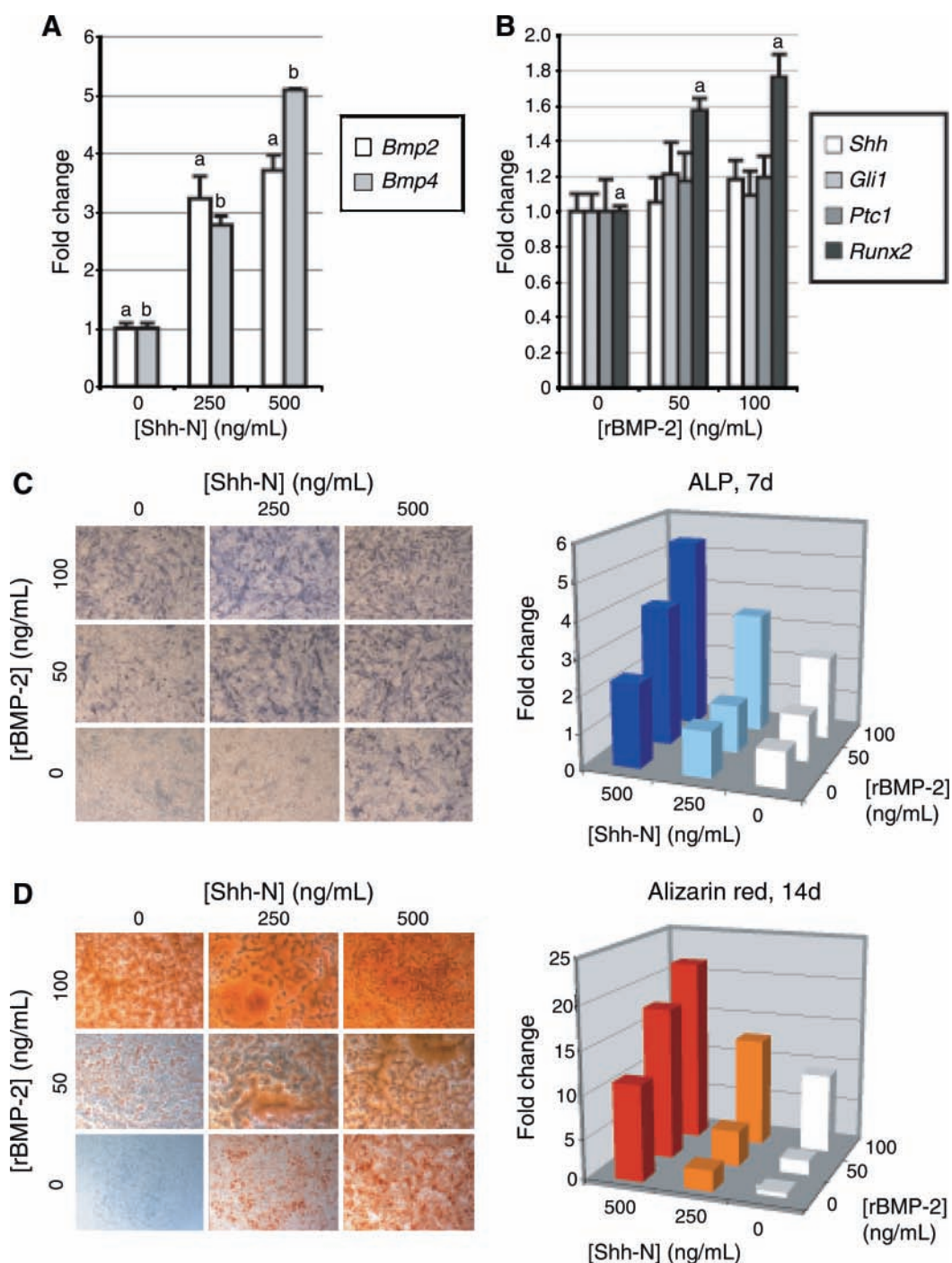


FIG. 5. Cooperation of Hedgehog and bone morphogenetic protein (BMP) signaling. (A) *Bmp2* and *Bmp4* expression after 48 h of Shh-N treatment, by qRT-PCR. (B) Hedgehog pathway activity after 48 h of recombinant (r)BMP-2 treatment, by qRT-PCR. (C) ALP staining (left) and quantification (right) after 7 days with Shh-N and/or rBMP-2. Bars represent mean ALP enzymatic activity, normalized to total protein content. (D) AR staining (left) and quantification (right) after 14 days with Shh-N and/or rBMP-2. Bars represent mean AR staining, as measured by absorbance after cetylpyridium chloride leaching. Photographs are of 20 \times magnification; values are normalized to control expression levels, ^{a,b} $p < 0.01$. Color images available online at www.liebertonline.com/ten.

which our laboratory has previously used to assess early defect healing.²¹ Using GFP immunostaining we confirmed that Shh-N and control-treated ASCs engrafted into the injury site (Fig. 6D, E). We found no difference in the volume of cells that engrafted (data not shown).

There was, however, a clear difference in the fate of grafted cells. mASCs exposed to Shh-N before transplantation showed significantly increased ALP activity (Fig. 6D, E, middle panel). Histomorphometric measurements of osteoid within the defect site showed that Shh-N-treated mASCs

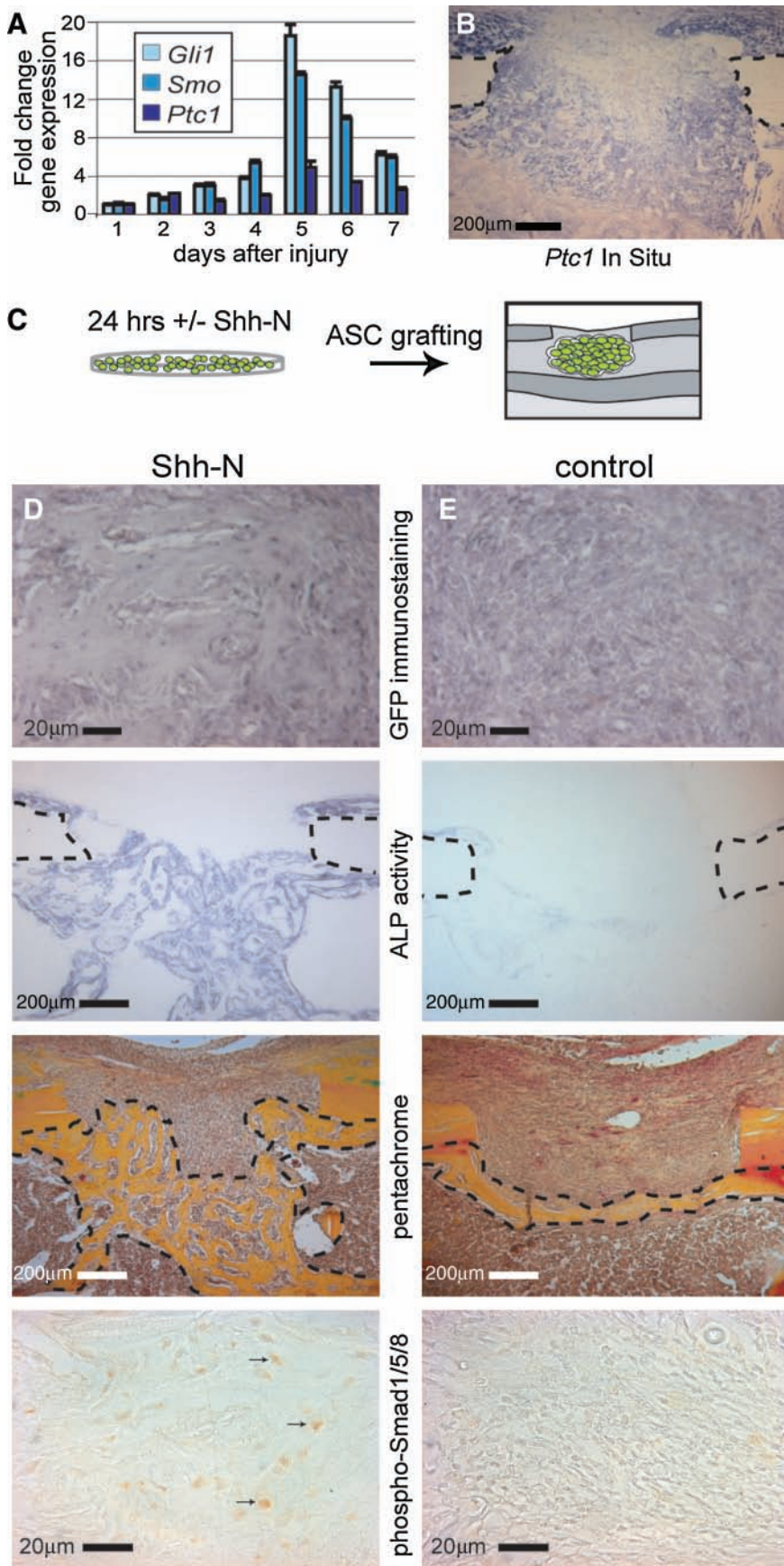


FIG. 6. Grafting of ASCs in tibial defects. **(A, B)** A 1-mm monocortical defect was surgically created in the proximal mouse tibia; spatiotemporal gene expression after injury was then examined by qRT-PCR and *in situ* hybridization. **(A)** Hedgehog signaling expression from 1 to 6 days postinjury (*Gli1*, *Smo*, and *Ptc1*). **(B)** *Ptc1* *in situ* in which positive staining cells appear purple; dotted lines demarcate the cortical bone. **(C)** Schematic of the grafting of green fluorescent protein (GFP)-positive ASCs into a monocortical tibial defect. **(D, E)** Histology of defects with Shh-N- or control-treated ASCs. From top to bottom, green fluorescent protein immunohistochemistry appearing gray, ALP staining appearing purple, pentachrome staining in which bone appears yellow, and phospho-Smad 1/5/8 immunohistochemistry appearing brown. Black arrows **D** indicate examples of positively stained cells for phospho-Smad 1/5/8. Color images available online at www.liebertonline.com/ten.

produced over 60% more bone than controls. Increased bone deposition among Shh-N-treated mASCs was associated with increased BMP activity, shown by immunohistochemistry for phospho-Smad 1/5/8 (Fig. 6D, E, bottom panel). Defects grafted with Shh-N-treated mASCs showed scattered positive staining within areas of bone regenerate, while little staining was observed among control-treated mASC-engrafted defects. Thus, in aggregate, exposing ASCs for a short time frame to exogenous Hedgehog protein enhanced osteoblast differentiation of the engrafted cells, resulting in increased bone deposition.

Discussion

Adipocytes and osteoblasts arise from a common progenitor,²² and as mammals age, the differentiation of adult stem cells appears to shift toward an adipogenic lineage at the expense of an osteoblastic fate.²³ This type of age-related change occurs in muscle satellite cells,²⁴ and in bone marrow.²⁵ In both stem cell populations, the acquisition of an adipogenic fate is due in part to activation of PPAR- γ .²⁶ PPAR- γ is a driving force for adipogenic differentiation, but it also appears to have an antiosteoblastic function.²⁷ Understanding the mechanisms that influence this balance between osteo- and adipogenesis is crucial to the future therapeutic use of ASCs for tissue regeneration.

While aging leads to an inevitable increase in fat at the expense of bone, our data suggest that this process can be influenced. The bipartite destiny of adult ASCs can be shifted away from an adipogenic and toward an osteogenic fate by exposure to the morphogen Shh. mASCs respond to Shh-N by upregulation of the master osteogenic transcription factor *Runx2* and, in turn, produce more ALP and exhibit significantly greater matrix mineralization (Fig. 3). The pro-osteogenic effect of Shh-N cannot be explained by an increase or expansion in the osteoprogenitor cell population (not seen by proliferation assays, data not shown), as has been postulated for other cytokines.²⁸ Rather, our data indicate that Shh-N accelerates the differentiation of osteoprogenitor mASCs.

Previous studies have examined the influence of age on the osteogenic capacity of ASCs, showing convincingly that age significantly attenuates human ASC (hASC) osteogenic differentiation,^{29,30} although this does not seem to be the case in mouse-derived cells.^{31,32} This dwindling osteogenic potential in hASCs with age has not been mechanistically defined, but does not appear to be due to a loss of osteoprogenitor cell numbers (as demonstrated by clonal analyses).³⁰ It is intriguing to speculate whether a decrease in endogenous Hedgehog signaling accompanies the decreasing osteogenic potential of hASCs with age. If true, the supplementation of Shh-N to ASCs *in vitro* may be of benefit in those cells derived from aged individuals.

Inhibition in Hedgehog signaling did not lead to cell death; instead, ASCs choose an adipogenic fate when exposed to the antagonist cyclopamine (Fig. 2). This is contrary to other reports showing that cyclopamine had no effect on preadipocyte cell lines and primary cell cultures.^{15,33} In our experiments, cyclopamine treatment led to a 35-fold increase in PPAR- γ expression (Fig. 2), which strongly argues against any direct cytotoxic effect for the alkaloid. Instead of inducing programmed cell death, cyclopamine significantly altered ASC differentiation.

Hedgehogs are not the only cytokines that alter ASC fate: BMPs and retinoic acid also induce osteogenesis in ASCs.^{5,17} Our data and others suggest that a combination of cytokines might be most advantageous for directing ASCs toward an osteoblast lineage.¹⁷ There are, however, clear challenges. First, potent morphogens are likely to have pleiotropic effects. For example, retinoic acid stimulates osteoclast activity,³⁴ which can be disadvantageous for bone repair. Second, some morphogens also act as mitogens.²⁸ Consequently, their duration of action and distribution of effect must be controlled. Third, numerous *in vitro* differences have been observed between mouse and human ASCs, including a capacity for more robust osteogenic differentiation in hASCs, and differential response to fibroblast growth factor, transforming growth factor- β , and BMP stimulation.^{5,35-38} A recent study has observed that Hedgehog signaling inhibits rather than promotes the osteogenic differentiation of hASCs.³⁹ Whether this discrepancy between our findings and others are due to differences in cell isolation, culture conditions, delivery of Hedgehog protein, or interspecies difference is not clear, and requires further investigation. Finally, there is the potential for interaction among exogenous and endogenous agents. Skeletal injury triggers activation of the Hedgehog (Fig. 6), Wnt,²¹ and BMP pathways. Whether these interactions are synergistic or antagonistic in the context of ASC-mediated bone repair remains to be determined.

ASCs are a readily available source of autologous tissue for repair and regeneration. Our data indicate that it is possible to combine ASCs and Shh-N in a therapeutic approach to accelerate bone regeneration. Do these data have a clinical application? The harvest of a patient's own adipose and its culture to expand the fraction of ASCs is currently achievable. One can imagine combining ASCs and a biomimetic scaffold that releases Shh-N to stimulate skeletal regeneration. Using autologous adult stem cells avoids the inherent complications associated with the introduction of nonautogenous stem cells, while reaching the end goal of restoring damaged or diseased tissues. Manipulation of Hedgehog signaling may prove advantageous toward this goal.

Acknowledgments

This study was supported by National Institutes of Health, National Institute of Dental and Craniofacial Research grants R21 DE-019274, and R01 DE-13194, the Hagey Foundation and the Oak Foundation to M.T.L.; National Institutes of Health, National Institute of Arthritis and Musculoskeletal and Skin Diseases grant IF32AR057302-01 to B.L.; Genentech Foundation Fellowship to A.W.J.; National Institutes of Health grants R01 PA-02-011, R01 AR-45-989 and Air Force Office of Research (FOS-2004-0025A) to J.A.H. We thank S. Washington for his excellent technical assistance.

Disclosure Statement

All authors have no conflicts of interest.

References

- Xu, Y., Malladi, P., Wagner, D.R., and Longaker, M.T. Adipose-derived mesenchymal cells as a potential cell source for skeletal regeneration. *Curr Opin Mol Ther* 7, 300, 2005.

2. Zuk, P.A., Zhu, M., Ashjian, P., De Ugarte, D.A., Huang, J.L., Mizuno, H., Alfonso, Z.C., Fraser, J.K., Benhaim, P., and Hedrick, M.H. Human adipose tissue is a source of multipotent stem cells. *Mol Biol Cell* **13**, 4279, 2002.
3. Nuttall, M.E., and Gimble, J.M. Controlling the balance between osteoblastogenesis and adipogenesis and the consequent therapeutic implications. *Curr Opin Pharmacol* **4**, 290, 2004.
4. Pei, L., and Tontonoz, P. Fat's loss is bone's gain. *J Clin Invest* **113**, 805, 2004.
5. Wan, D.C., Shi, Y.Y., Nacamuli, R.P., Quarto, N., Lyons, K.M., and Longaker, M.T. Osteogenic differentiation of mouse adipose-derived adult stromal cells requires retinoic acid and bone morphogenetic protein receptor type IB signaling. *Proc Natl Acad Sci USA* **103**, 12335, 2006.
6. Villavicencio, E.H., Walterhouse, D.O., and Iannaccone, P.M. The sonic hedgehog-patched-gli pathway in human development and disease. *Am J Hum Genet* **67**, 1047, 2000.
7. Borycki, A., Brown, A.M., and Emerson, C.P., Jr. Shh and Wnt signaling pathways converge to control Gli gene activation in avian somites. *Development* **127**, 2075, 2000.
8. Neumann, C.J. Hedgehogs as negative regulators of the cell cycle. *Cell Cycle* **4**, 1139, 2005.
9. Spinella-Jaegle, S., Rawadi, G., Kawai, S., Gallea, S., Faucheu, C., Mollat, P., Courtois, B., Bergaud, B., Ramez, V., Blanchet, A.M., Adelmant, G., Baron, R., and Roman-Roman, S. Sonic hedgehog increases the commitment of pluripotent mesenchymal cells into the osteoblastic lineage and abolishes adipocytic differentiation. *J Cell Sci* **114**, 2085, 2001.
10. Kasper, M., Regl, G., Frischauf, A.M., and Aberger, F. Gli transcription factors: mediators of oncogenic hedgehog signalling. *Eur J Cancer* **42**, 437, 2006.
11. van der Horst, G., Farih-Sips, H., Lowik, C.W., and Karperien, M. Hedgehog stimulates only osteoblastic differentiation of undifferentiated KS483 cells. *Bone* **33**, 899, 2003.
12. Jemtland, R., Divieti, P., Lee, K., and Segre, G.V. Hedgehog promotes primary osteoblast differentiation and increases PTHrP mRNA expression and iPTHrP secretion. *Bone* **32**, 611, 2003.
13. Yuasa, T., Kataoka, H., Kinto, N., Iwamoto, M., Enomoto-Iwamoto, M., Iemura, S., Ueno, N., Shibata, Y., Kurosawa, H., and Yamaguchi, A. Sonic hedgehog is involved in osteoblast differentiation by cooperating with BMP-2. *J Cell Physiol* **193**, 225, 2002.
14. Nakamura, T., Aikawa, T., Iwamoto-Enomoto, M., Iwamoto, M., Higuchi, Y., Pacifici, M., Kinto, N., Yamaguchi, A., Noji, S., Kurisu, K., and Matsuya, T. Induction of osteogenic differentiation by hedgehog proteins. *Biochem Biophys Res Commun* **237**, 465, 1997.
15. Fontaine, C., Cousin, W., Plaisant, M., Dani, C., and Peraldi, P. Hedgehog signaling alters adipocyte maturation of human mesenchymal stem cells. *Stem Cells* **26**, 1037, 2008.
16. Suh, J.M., Gao, X., McKay, J., McKay, R., Salo, Z., and Graff, J.M. Hedgehog signaling plays a conserved role in inhibiting fat formation. *Cell Metab* **3**, 25, 2006.
17. Malladi, P., Xu, Y., Yang, G.P., and Longaker, M.T. Functions of vitamin D, retinoic acid, and dexamethasone on mouse adipose-derived mesenchymal cells (AMCs). *Tissue Eng* **12**, 2031, 2006.
18. James, A.W., Xu, Y., Wang, R., and Longaker, M.T. Proliferation, osteogenic differentiation, and fgf-2 modulation of posterofrontal/sagittal suture-derived mesenchymal cells *in vitro*. *Plast Reconstr Surg* **122**, 53, 2008.
19. Leucht, P., Kim, J.B., Amasha, R., James, A.W., Girod, S., and Helms, J.A. Embryonic origin and Hox status determine progenitor cell fate during adult bone regeneration. *Development* **135**, 2845, 2008.
20. Brugmann, S.A., Allen, N.C., James, A.W., Mekonnen, Z., Madan, E., and Helms, J.A. A primary cilia-dependent etiology for midline facial disorders. *Hum Mol Genet* **19**, 1577, 2010.
21. Kim, J.B., Leucht, P., Lam, K., Luppen, C., Ten Berge, D., Nusse, R., and Helms, J.A. Bone regeneration is regulated by wnt signaling. *J Bone Miner Res* **22**, 1913, 2007.
22. Uccelli, A., Moretta, L., and Pistoia, V. Mesenchymal stem cells in health and disease. *Nat Rev Immunol* **8**, 726, 2008.
23. Bianco, P., Riminucci, M., Gronthos, S., and Robey, P.G. Bone marrow stromal stem cells: nature, biology, and potential applications. *Stem Cells* **19**, 180, 2001.
24. Taylor-Jones, J.M., McGehee, R.E., Rando, T.A., Lecka-Czernik, B., Lipschitz, D.A., and Peterson, C.A. Activation of an adipogenic program in adult myoblasts with age. *Mechanisms of ageing and development* **123**, 649, 2002.
25. Moerman, E.J., Teng, K., Lipschitz, D.A., and Lecka-Czernik, B. Aging activates adipogenic and suppresses osteogenic programs in mesenchymal marrow stroma/stem cells: the role of PPAR-gamma2 transcription factor and TGF-beta/BMP signaling pathways. *Aging Cell* **3**, 379, 2004.
26. Kirkland, J.L., Tchkonina, T., Pirtskhalava, T., Han, J., and Karagiannides, I. Adipogenesis and aging: does aging make fat go MAD? *Exp Gerontol* **37**, 757, 2002.
27. Lin, T.H., Yang, R.S., Tang, C.H., Lin, C.P., and Fu, W.M. PPARgamma inhibits osteogenesis via the down-regulation of the expression of COX-2 and iNOS in rats. *Bone* **41**, 562, 2007.
28. Quarto, N., and Longaker, M.T. FGF-2 inhibits osteogenesis in mouse adipose tissue-derived stromal cells and sustains their proliferative and osteogenic potential state. *Tissue Eng* **12**, 1405, 2006.
29. de Girolamo, L., Lopa, S., Arrigoni, E., Sartori, M.F., Baruffaldi Preis, F.W., and Brini, A.T. Human adipose-derived stem cells isolated from young and elderly women: their differentiation potential and scaffold interaction during *in vitro* osteoblastic differentiation. *Cytotherapy* **11**, 793, 2009.
30. Zhu, M., Kohan, E., Bradley, J., Hedrick, M., Benhaim, P., and Zuk, P. The effect of age on osteogenic, adipogenic and proliferative potential of female adipose-derived stem cells. *J Tissue Eng Regen Med* **3**, 290, 2009.
31. Shi, Y.Y., Nacamuli, R.P., Salim, A., and Longaker, M.T. The osteogenic potential of adipose-derived mesenchymal cells is maintained with aging. *Plast Reconstr Surg* **116**, 1686, 2005.
32. Yamada, T., Akamatsu, H., Hasegawa, S., Yamamoto, N., Yoshimura, T., Hasebe, Y., Inoue, Y., Mizutani, H., Uzawa, T., Matsunaga, K., and Nakata, S. Age-related changes of p75 Neurotrophin receptor-positive adipose-derived stem cells. *J Dermatol Sci* **58**, 36, 2010.
33. Cousin, W., Dani, C., and Peraldi, P. Inhibition of the anti-adipogenic Hedgehog signaling pathway by cyclopamine

- does not trigger adipocyte differentiation. *Biochem Biophys Res Commun* **349**, 799, 2006.
34. Gautschi, O.P., Frey, S.P., and Zellweger, R. Bone morphogenetic proteins in clinical applications. *ANZ J Surg* **77**, 626, 2007.
 35. Grewal, N.S., Gabbay, J.S., Ashley, R.K., Wasson, K.L., Bradley, J.P., and Zuk, P.A. BMP-2 does not influence the osteogenic fate of human adipose-derived stem cells. *Plast Reconstr Surg* **123**, 158S, 2009.
 36. Dragoo, J.L., Choi, J.Y., Lieberman, J.R., Huang, J., Zuk, P.A., Zhang, J., Hedrick, M.H., and Benhaim, P. Bone induction by BMP-2 transduced stem cells derived from human fat. *J Orthop Res* **21**, 622, 2003.
 37. Quarto, N., Wan, D.C., and Longaker, M.T. Molecular mechanisms of FGF-2 inhibitory activity in the osteogenic context of mouse adipose-derived stem cells (mASCs). *Bone* **42**, 1040, 2008.
 38. Levi, B., James, A.W., Xu, Y., Commons, G.W., and Longaker, M.T. Divergent modulation of adipose-derived stromal cell differentiation by TGF-beta1 based on species of derivation. *Plast Reconstr Surg*, 2010 (In press).
 39. Plaisant, M., Fontaine, C., Cousin, W., Rochet, N., Dani, C., and Peraldi, P. Activation of hedgehog signaling inhibits osteoblast differentiation of human mesenchymal stem cells. *Stem Cells* **27**, 703, 2009.

Address correspondence to:

Michael T. Longaker, M.D., M.B.A.
Hagey Pediatric Regenerative Medicine Laboratory
Division of Plastic and Reconstructive Surgery
Department of Surgery
Stanford University School of Medicine
257 Campus Drive
Stanford, CA 94305-5148

E-mail: longaker@stanford.edu

Jill A. Helms, Ph.D., D.D.S.
Hagey Pediatric Regenerative Medicine Laboratory
Division of Plastic and Reconstructive Surgery
Department of Surgery
Stanford University School of Medicine
257 Campus Drive
Stanford, CA 94305-5148

E-mail: jhelms@stanford.edu

Received: January 26, 2010

Accepted: March 26, 2010

Online Publication Date: May 20, 2010